NanoPDLIM2 enhanced efficacy of PD-1 blockade and chemotherapy in mouse lung cancers

Fan Sun[1], Pengrong Yan[1], Yadong Xiao[1, 2, 3, 4], Hongqiao Zhang[3], Steven D. Shapiro[2, 4], Gutian Xiao[1, 3, *], and Zhaoxia Qu[1, 3, *]

[1]UPMC Hillman Cancer Center, Department of Microbiology and Molecular Genetics, University of Pittsburgh School of Medicine, Pittsburgh, PA 15213, USA. [2]Division of Pulmonary, Allergy, and Critical Care Medicine, Department of Medicine, University of Pittsburgh School of Medicine, Pittsburgh, PA 15213, USA. [3]Norris Comprehensive Cancer Center, Hastings Center for Pulmonary Research, Department of Molecular Microbiology and Immunology, University of Southern California Keck School of Medicine, Los Angeles, CA 90033, USA. [4]Department of Medicine, University of Southern California Keck School of Medicine, Los Angeles, CA 90033, USA.

[*]Correspondence should be addressed to Zhaoxia Qu (Email: Zhaoxia.Qu@med.usc.edu; Phone: 323-442-6932) or Gutian Xiao (Email: Gutian.Xiao@med.usc.edu; Phone: 323-442-7985)

Running Title: NanoPDLIM2-chemo-immuno-therapy in lung cancer

Keywords: PD-1; PDLIM2; immune checkpoint; ICIs; nanotherapy; combination therapy; lung cancer; preclinical studies; mouse models

Disclosure of Potential Conflicts of Interest: The authors declare no potential conflicts of interest.

Abstract

Background: Immune checkpoint inhibitors (ICIs) and their combination with other therapies such as chemotherapy, fail in most cancer patients. We previously identified the PDZ-LIM domain-containing protein 2 (PDLIM2) as a *bona fide* tumor suppressor that is repressed in lung cancer to drive cancer and its chemo- and immunotherapy resistance, suggesting a new target for lung cancer therapy improvement.

Methods: Human clinical samples and data were used to investigate *PDLIM2* genetic and epigenetic changes in lung cancer. Using an endogenous mouse lung cancer model faithfully recapitulating refractory human lung cancer and a clinically feasible nano-delivery system, we investigated the therapeutic efficacy, action mechanism, and safety of systemically administrated *Pdlim2* expression plasmids encapsulated in nanoparticles (nanoPDLIM2) and its combination with PD-1 antibody and chemotherapeutic drugs.

Results: *PDLIM2* repression in human lung cancer involves both genetic deletion and promoter methylation. NanoPDLIM2 showed low toxicity, high tumor specificity, antitumor activity, and greatly improved the efficacy of anti-PD-1 and chemotherapeutic drugs, with complete tumor remission in 60% of mice and substantial tumor reduction in the remaining mice by the combination of three therapies. Mechanistically, nanoPDLIM2 increased major histocompatibility complex class I (MHC-I) expression, suppressed multi-drug resistance 1 (MDR1) induction, nuclear Rela and stat 3, and survival genes (Bcl-xl and cycline D1) in tumor cells; meanwhile it enhanced lymphocyte tumor infiltration and activation, thus turning the cold tumors hot and sensitive to ICIs and rendering them vulnerable to chemotherapeutic drugs.

Conclusions: These studies established a clinically applicable PDLIM2-based combination therapy with significantly improved efficacy for lung cancer and possibly other cold cancers.

Introduction

Lung cancer is the leading cause of cancer-related deaths in both men and women with a 5-year survival rate of only 22% [1]. Although these outcomes may be improved by immune checkpoint blockade therapy involving the disruption of the binding of programmed cell death 1 (PD-1, also known as CD279) on tumor-infiltrating lymphocytes (TILs) to programmed death receptor ligand 1 (PD-L1, also known as B7-H1 or CD274) on tumor and tumor-associated cells, most lung cancer patients still fail the therapy, with a response rate of only about 20% [2]. In general, this revolutionary immunotherapy works better against 'hot' tumors, which have abundant TILs in the tumor microenvironment, strong immunogenicity and sufficient PD-L1 expression on cancer cells. Unfortunately, most tumors are 'cold', with low T-cell infiltration, weak immunogenicity and minimal PD-L1 expression, and show weak response to immune checkpoint inhibitors (ICIs) [3, 4].

Cold lung tumors without targetable oncogenic drivers are treated with chemotherapy as the standard approach [5]. However, the response rate to this conventional cancer therapy is also low and resistance often occurs after an initial response, with an overall survival (OS) of about 12-17 months. Given its roles of inducing TILs and immunogenicity, in particular PD-L1 expression, chemotherapy can be an ideal candidate for combination with PD-1/PD-L1 blockade to improve therapeutic efficacy [6]. Indeed, combination treatment with ICIs and chemotherapeutic drugs shows synergy and better efficacy in both preclinical animal models and clinical trials of lung cancer and other cancers [6-8]. However, even with the combination of ICIs and chemotherapy, tumors in animals do not remit completely and the objective response rate (ORR) of lung cancer patients only reaches 33%-49.7%, with a median progression-free survival (PFS) of just 5.1-9 months and a median OS of 13-22 months [7, 8]. Thus, further improvement over the chemo-immunotherapy is direly need.

Our recent studies on human and animal lung cancers have shown that most lung tumors not only have

low TILs and decreased PD-L1, but also down-regulate major histocompatibility complex class I (MHC-I), thus evading recognition and attack by $CD8^+$ T cells, including those unleashed by ICIs and/or recruited by chemotherapy [6, 9, 10]. Following our initial studies [11-17], we have established the PDZ-LIM domain-containing protein *PDLIM2*, also known as SLIM or mystique [18-20], as a *bona fide* tumor suppressor, and its repression is a causative driver of lung cancer and resistance to ICIs and chemotherapeutic agents [6]. One most important function of PDLIM2 is to promote the ubiquitination and proteasomal degradation of nuclear signal transducer and activator of transcription 3 (STAT3) and nuclear factor-κB (NF-κB) RelA (also known as p65), two master transcription factors that function as proto-oncogenes in lung and many other cancers [6, 10-13, 21-27]. *Pdlim2* repression in tumor cells thus results in the persistent activation of Stat3 and Rela, leading to MHC-I downregulation and high expression of tumor growth-related genes [6]. In addition, *Pdlim2* deficiency also causes strong induction of multi-drug resistance 1 (MDR1) for acquired chemo-resistance [6]. Therefore, *PDLIM2* is a potential target to further enhance the efficacy of chemo-and immune-therapies for lung cancers.

In this study, we explored the mechanism of *PDLIM2* repression in human lung cancers and tested whether systemic administration of nanoparticle-encapsulated *Pdlim2*-expression plasmids (nanoPDLIM2) could enhance the efficacy of anti-PD-1 and/or chemotherapeutic drugs in a mouse lung cancer model. These studies indicate that besides epigenetic repression, loss of heterozygosity (LOH) with copy number losses contributes to *PDLIM2* downregulation in about 58% of human lung cancers, and that *Pdlim2* heterozygous deletion ($Pdlim2^{+/-}$) mice develop spontaneous tumors in lung and other organs. Notably, systemic administration of nanoPDLIM2 reverses the phenotypes caused by *Pdlim2* repression in lung tumors, and its combination with PD-1 and chemotherapeutic drugs shows the strongest therapeutic efficacy compared to single or double therapies, inducing complete remission of lung tumors in 60% of mice. These findings provide a firm basis to target *PDLIM2* to enhance the efficacy of ICIs and chemotherapeutic drugs for lung cancer therapy.

Material and Methods

Animals and lung carcinogenesis

We have complied with all relevant ethical regulations for animal testing and research. The animal experiments were performed in accordance with the US National Institutes of Health (NIH) Guidelines on the Use of Laboratory Animals. All animals were maintained under pathogen-free conditions and used according to protocols approved by the Institutional Animal Care and Use Committee (IACAUC) of the University of Pittsburgh. *Pdlim2*$^{flx/flx}$/*Spc*-rtTA$^{tg/-}$/(tetO)7CMV-Cre$^{tg/tg}$ (ΔSPC) mice under a pure FVB/N background and *Pdlim2*$^{-/-}$ mice under a pure BALB/c background have been described before [6, 19, 21, 22, 28]. For lung carcinogenesis, six- to eight-week-old ΔSPC and wild type FVB/N mice were intraperitoneally (i.p.) injected with urethane (1 mg/g body weight, Sigma-Aldrich, St. Louis, MO, USA) once a week for six consecutive weeks [6], followed by different treatments as shown in the figures. Mice were sacrificed at six weeks post urethane treatment for examination of lung tumors, inflammation, and treatment-induced toxicity. Surface tumors in mouse lungs were counted blinded under a dissecting microscope, and tumor diameters were measured by microcalipers.

Preparation of *Pdlim2*-expression plasmid or empty vector plasmid nanoparticles

The polyethylenimine (PEI)-based nanoparticles (*in vivo*-jetPEI) (Polyplus Transfection, New York, NY, USA) and plasmid DNA complexes at a nitrogen-to-phosphate ratio of 8 (N/P=8) were prepared according to the manufacturer's instructions. Briefly, 25 μg of pCMV-myc-*Pdlim2* [21] or empty vector plasmids in 100 μl of a 5% glucose solution were mixed with the *in vivo*-jetPEI reagent (4 μl) diluted into 100 μl of a 5% glucose solution. After 15 minutes of incubation at room temperature, the mixed solution (200 μl/mouse) was injected intravenously (i.v.) via the tail vein. Presence of nanoPDLIM2 in tissues were measured by PCR assays targeting Amp-R and Lyz2 in the genome of empty vector and *Pdlim2* plasmids.

Histology and immunohistochemistry (IHC) analysis

Lung, liver, kidney, and spleen tissues were excised, fixed in formalin, embedded in paraffin, and cut into 4-μm-thick sections. Sections were stained with H&E, or subjected to sequential incubations with the indicated primary antibodies, biotinylated secondary antibodies and streptavidin-HRP [6]. Antibodies were listed in Supplementary Table S1.

***In vivo* BrdU labeling**

Mice were i.p. injected with 50 mg/kg BrdU (Sigma-Aldrich, St. Louis, MO, USA) 24 h prior to sacrifice. Mouse lung tissue sections were stained with anti-BrdU (Sigma-Aldrich, St. Louis, MO, USA). BrdU labeling index was calculated as the percentage of labeled cells per total cells counted (> 500 cells in each counted tumor-containing area).

Flow cytometry (FACS) analysis

The cells were isolated from mouse lungs using dispase digestion followed filtration with 70 μm Nylon cell strainer; then cells were incubated with the antibodies against cell surface antigens after blocked with αCD16/CD32. The cells were then fixed with paraformaldehyde (2%), permeabilized and incubated with antibodies against intracellular antigens if needed. For interferon-γ (IFNγ) staining, cells were treated with phorbol 12-myristate 13-acetate (PMA, 50 ng/ml), ionomycin (1 μM), brefeldin A (BFA, 3 μg/ml) and monensin (2 μM) for 4 h before they were stained for FACS analysis. Data were acquired and analyzed by Accuri C6 or LSRFortessa I (BD Biosciences) and FlowJo software [29].

Quantitative polymerase chain reaction (qPCR) analysis

The indicated tissues or cells were subjected to DNA or RNA extraction, RNA reverse transcription and real-time PCR using trizol, reverse transcriptase, and Power SYBR Green PCR Master Mix (Thermo

Fisher Scientific, Waltham, MA USA) according to manufacturer's protocol. Primer pairs used for qPCR were listed in Supplementary Table S2.

Microsatellite and gene-specific PCR-based LOH analysis of *PDLIM2*

Genomic DNAs were isolated from human lung tumors and their matched normal tissues using the PureLink Genomic DNA Purification Kit (Invitrogen, Carlsbad, CA, USA), and subjected to semi-quantitative PCR using the primers specific for the microsatellite markers D8S1786 and D8S1752 that straddle the *PDLIM2* genetic locus or the *PDLIM2* genetic locus itself. Primer pairs used for the assays were listed in Supplementary Table S2.

Statistical analysis

One-way ANOVA power analysis was used to determine the minimum sample size. Animals were randomly assigned to different treatment groups. Measurements were taken from distinct samples. Student's t test (two tailed) and one-way ANOVA/Tukey's or two-way ANOVA/Sidak's test were used to assess significance of differences between two groups and multiple comparisons, respectively. Pearson's correlation test was used to assess association between *PDLIM2* expression with its promoter methylation or genetic deletion and the overlap between *PDLIM2* promoter methylation and genetic deletion. All bars in figures represent means ± standard error of the mean (SEM). The p values are indicated as $*p < 0.05$, $**p < 0.01$, ns, not statistically significant, except for those shown in figures. The p values < 0.05 and 0.01 are considered statistically significant and highly statistically significant, respectively. Grubbs' and ROUT outlier tests were established a priori. There were no exclusions in the analyses.

Results

Both epigenetic repression and genetic deletion of *PDLIM2* in lung cancer

Using 40% of the expression level of matched normal lung tissues as the cut-off, *PDLIM2* was repressed in over 75% of human lung cancers in a prior study [6]. Analysis of the Cancer Genome Atlas (TCGA) database found that if using 50% as the cut-off, *PDLIM2* was repressed in about 93% of human lung cancers (Figure 1*A*). Further analysis of the TCGA dataset showed that over 70% of human lung cancers with decreased *PDLIM2* expression had hypermethylation in *PDLIM2* promoter, when using 125% of the methylation level of the *PDLIM2* promoter in normal lung tissues as the cut-off (Figure 1*A*, 1*B*), validating our previous finding that epigenetic silencing was the main mechanism underlying *PDLIM2* repression in lung cancer [6].

In line with *PDLIM2*'s location on chromosome 8p21.3, a frequent LOH region in lung and other tumors [30-34], analysis of the TCGA database revealed that *PDLIM2* expression was positively associated with its gene copy numbers, and that over 58% of human lung cancers with decreased *PDLIM2* expression had genetic deletion of the *PDLIM2* gene if copy number variation (CNV) of -0.1 was used as the cut-off for the gene deletion (Figure 1*C*). Further analysis indicated that about 44% of human lung cancers with decreased *PDLIM2* expression simultaneously harbored the promoter hypermethylation and LOH with copy number losses of the *PDLIM2* gene, and approximately 26% and 14% of them only having the promoter hypermethylation and LOH, respectively (Figure 1*D*). The gene deletion of *PDLIM2* was confirmed by microsatellite and gene-specific PCR-based LOH analysis of human primary lung cancer tissues and cell lines (Figure 1*E*, 1*F*; Supplementary Table S3). These data suggested that *PDLIM2* repression in lung cancer involves both epigenetic silencing and genetic deletion.

To determine the significance of *PDLIM2* LOH in lung tumor, we examined whether *Pdlim2* heterozygous deletion leads to decreased *Pdlim2* expression and spontaneous tumors in mice. Unlike its absolute absence in *Pdlim2* homozygous deletion (*Pdlim2*$^{-/-}$) mice, Pdlim2 was detected in the lung of *Pdlim2*$^{+/-}$ mice, but at a much lower level compared to wild type (WT) mice (about 50% of WT, Supplementary

Figure S1*A*). Importantly, *Pdlim2*$^{+/-}$ mice, like *Pdlim2*$^{-/-}$ mice, also developed spontaneous tumors (Figure 1*G*). Of note, over 50% of tumors developed in *Pdlim2*$^{-/-}$ and *Pdlim2*$^{+/-}$ mice were lung tumors (Figure 1*H*; Supplementary Figure S1*B*). These data are also highly consistent with the fact that *PDLIM2* is ubiquitously expressed under physiological conditions, with the highest level in the lung and lung epithelial cells in particular [6, 18-20]. Thus, *PDLIM2* is a haploinsufficient tumor suppressor that is particularly important for lung tumor suppression**.**

Efficacy of systemic administration of nanoPDLIM2 in refractory lung cancer

Although reversal of *PDLIM2* epigenetic repression by epigenetic drugs to restore *PDLIM2* expression in cancer cells may be used to treat lung cancers [6], this approach cannot be applied to lung cancers involving *PDLIM2* LOH with copy number losses, as occurred in 58% of all lung cancer cases. To overcome this limitation and expand *PDLIM2*-targeted therapy to all lung cancers with *PDLIM2* repression, we tested the therapeutic efficacy of systemic administration of *PDLIM2*-expression plasmids encapsulated by the clinically feasible *in vivo*-jetPEI [35-39]. To this end, we employed mouse lung cancers induced by urethane, a faithful model of human lung cancer and adenocarcinoma (AC) in particular [6, 23, 24, 40-43]. Urethane is a chemical carcinogen present in fermented food, alcoholic beverage and also cigarette smoke, the predominant risk factor accounting for about 90% of human lung cancers [44]. Like its human counterpart, the murine lung cancer induced by urethane also shares *Pdlim2* repression, in addition to their similarities in histology, genetics, molecular biology and immunology [6, 9, 23, 24, 40-43]. WT mice with lung tumors induced by urethane were i.v. injected with nanoparticle-encapsulated *Pdlim2* plasmids or empty vector plasmids. Six weeks post the initial treatment of nanoPDLIM2, mice were sacrificed and lung tissues were collected for assays (Figure 2*A*). Compared to the empty vector plasmid mock-treated group (Vec), nanoPDLIM2-treated mice had a significantly reduced tumor burden (-31%) in their lungs, though the response of tumor numbers was weak (Figure 2*B*).

In line with the reduction in tumor burden, nanoPDLIM2 administration decreased nuclear Rela and Stat3, a hallmark of NF-κB and STAT3 activation, accordingly reduced the expression of their downstream cell survival gene *Bcl2l1*(Bcl-xl, -49%) and cell proliferation gene Ccnd1 (Cyclin D1, -61%), increased cleaved caspase 3 (+230%), a marker of apoptosis, and decreased proliferation (-47%) of lung cancer cells (Figure 2*C*-2*E*). These data indicated that intravenous administration of nanoPDLIM2 reduced lung tumor burden, suppressed oncogenic Rela and Stat3 activation and increased apoptosis of lung tumors.

High tumor specificity and low toxicity of systemic administration of nanoPDLIM2

To characterize the efficiency of systemically administrated nanoPDLIM2, we examined *Pdlim2* expression in lung tumors and several organs, including the liver, kidney and spleen. A high level of Pdlim2 was detected in the lung tumors from mice treated with nanoPDLIM2 one week post the injection, whereas no obvious Pdlim2 was detected in the lung tumors from mice of Vec group (Figure 3*A*, 3*B*). It should be pointed out that the tumor delivery efficiency of *Pdlim2*-expression or empty vector plasmid nanoparticles did not differ (Figure 3*B*). However, either *Pdlim2*-expression or empty vector plasmids were hardly detected in other organs/tissues of the same mice, including liver, kidney and spleen (Figure 3*B*). Of note, in the first two days after injection, both empty vector and *Pdlim2* plasmids were also detected at high levels in those tissues but quickly declined afterward (data not shown), consistent with the well-documented tumor-specific enrichment of nanoparticles [37, 45-47]. Consistently, ectopic Pdlim2 was not detected, and the levels of *Pdlim2* protein were comparable in these tissues (Figure 3*B*, 3*C*).

The i.v. injection of either Pdlim2-expression or control plasmid nanoparticles showed no obvious toxicity to animals, as evidenced by no significant changes in body weight and histology of all organs/tissues examined, including the spleen, kidney and liver (Figure 3*D*, *E*). Mouse appearance and behaviors, such as eating, drinking, defecating, urinating, sniffing, grooming and digging, were not different between

control and nanoparticle groups (data not shown). Taken together, these data suggest nanoPDLIM2 shows therapeutic efficacy in the mouse lung tumor model while causes low toxicity.

Synergy of nanoPDLIM2 with chemotherapy in lung cancer treatment

Given the role of *Pdlim2* in inhibiting the expression of cell survival and proliferation genes in tumor cells, which contribute to chemoresistance, we tested whether nanoPDLIM2 increases the efficacy of chemotherapy in the mouse model of lung cancer. Treatment with carboplatin and paclitaxel, two first-line chemotherapeutic drugs for lung and many other cancers, led to a significant decrease in tumor number (-35%) and tumor burden (-87%) (Figure 4*A*). Importantly, combination with nanoPDLIM2 further decreased both tumor number (-78%) and tumor burden (-94%), suggesting a promising synergy between nanoPDLIM2 and chemotherapy in lung cancer treatment. Consistently, significantly higher tumor cell apoptosis was detected in mice treated with the combination therapy (+650%), in comparison to those with nanoPDLIM2 (+200%) or chemotherapy (+230%) alone (Figure 4*B*).

Chemotherapy induced strong Rela activation/nuclear expression and *Mdr1* expression (Figure 4*C*, 4*D*). NanoPDLIM2 not only repressed the constitutive activation of Rela in cancer cells but also prevented the strong induction of Rela activation and Mdr1 expression by the chemotherapy. Thus, nanoPDLIM2 improves the therapeutic efficacy of chemotherapy through blocking both intrinsic and acquired chemoresistance of lung cancer cells.

NanoPDLIM2 enhanced the efficacy of ICIs in lung cancer treatment

High expression of cell survival genes renders tumor cells resistant to the tumoricidal activity of cytotoxic T lymphocytes (CTLs), including those unleashed by ICIs. Given nanoPDLIM2 administration suppressed survival genes in lung tumors (Figure 2*E*), we hypothesize it enhances the efficacy of immunotherapy. NanoPDLIM2 increased the number of TILs and the expression of MHC-I, the most

important and core components of immunotherapies including PD-1 immune checkpoint blockade therapy (Figure 5*A*, 5*B*). In line with our previous studies [6], PD-1 blocking antibody reduced tumor burden (-25%) and tumor number (-13%) (Figure 5*C*). Combining with PDLIM2 nanotherapy further decreased tumor burden (-64%), and caused a trend toward decrease for tumor number. Consistently, higher increases in both $CD4^+$ and $CD8^+$ TILs, stronger $CD8^+$ CTL activation and lung tumor cell death were detected in combination therapies of nanoPDLIM2 and PD-1 antibody (Figure 5*D*-5*F*). These data together suggest that nanoPDLIM2 enhanced the therapeutic efficacy of PD-1 blockade.

Complete remission of all lung cancers in most mice by the combination treatment of nanoPDLIM2 and anti-PD-1 and chemotherapeutic drugs

Like most human lung cancers, lung cancers in our animal model exhibit a decreased expression of PD-L1 on cell surface, in additional to the low expression of MHC-I and low number of TILs [6, 9]. In line with our previous finding that PD-L1 expression is largely independent of *Pdlim2* [6], nanoPDLIM2 failed to induce PD-L1 expression in lung tumors; in contrast, chemotherapy induced PD-L1 (Figure 6*A*). This may explain why the enhancing effect of nanoPDLIM2 on PD-1 blockade therapy is only moderate.

Induction of PD-L1 could protect cancer cells from immune attack and thereby restricts further efficacy improvement from its combination with PDLIM2 nanotherapy, which increased TILs (Figure 4*A*); on the other hand, upregulated PD-L1 may increase the sensitivity of cancer cells to PD-1 blockade therapy. Indeed, combination of chemotherapeutic drugs and PD-1 blockade showed a promising synergy in reducing both tumor number and tumor burdens in comparison to the individual treatment of chemotherapy or PD-1 blockade therapy [6]. The synergy was largely blocked when *Pdlim2* was genetically deleted from lung cancer cells (ΔSPC) (Figure 6*B*, 6*C*), suggesting an important role of *Pdlim2* in the combination therapy of chemotherapeutic drugs and anti-PD-1. Whereas *PDLIM2 nanotherapy* increased MHC-I expression on tumor cells (Figure 5*B*), which is critical for better recognition and killing

of tumor cells by $CD8^+$ CTLs, chemotherapy alone or its combination with anti-PD-1 failed to do so (Figure 6*D*). Accordingly, combination of anti-PD-1 and chemotherapeutic drugs, like the combination therapies of nanoPDLIM2 and anti-PD-1 or chemotherapeutic drugs, also failed to induce a complete remission of lung cancers in any mice.

Given their overlapping roles in increasing TILs and in particular their complement roles in inducing MHC-I and PD-L1 expression on tumor cells, which turn tumors hot and more sensitive to PD-1 blockade, better efficacy is expected for combination of nanoPDLIM2, chemotherapeutic drugs, and anti-PD-1 compared to single therapy or combination of double therapies. Indeed, combination of the three showed the strongest effect on reducing tumor burden and numbers, and caused complete remission of lung cancers in 60% of mice (Figure 6*E*) and much more shrinkage of lung tumors in remaining mice in comparison to those treated with two combined therapies (data not shown). In line with the increase in therapeutic efficacy, the triple combination therapy significantly increased the numbers and/or activation of $CD4^+$ and $CD8^+$ T cells in the lung, compared to the combination of chemotherapeutic drugs and anti-PD-1 (Figure 6*F*, 6G).

Of note, consistent with the undetectable toxicity of *PDLIM2 nanotherapy*, its co-treatment did not further increase the toxicity of anti-PD-1 and chemotherapeutic drugs, as evidenced by no obvious histological difference of major organs, including the liver, lung, kidney, and spleen (Supplementary Figure S2), and no significant differences in animal body weights, in comparison to the mice received the combinational treatment of anti-PD-1 and chemotherapeutic drugs in the presence or absence of empty vector plasmid nanoparticles (Figure 6*H*).

Discussion

PD-1/PD-L1 blockade immunotherapy has recently joined chemotherapy as a standard treatment for lung

and several other cancers [2-4]. While some patients have shown dramatic responses, most patients do not benefit from this novel treatment. Currently, various combinations of ICIs with other therapies, in particular with chemotherapeutic drugs, are being extensively tested in both preclinical and clinical trial studies, aiming to expand the benefit of this innovative therapy [6-8]. Although a promising synergy and better efficacy have been observed in some of these studies [6-8], further improvement is direly needed. Using a mouse model of lung cancer, we show, for the first time, that PDLIM2 *nanotherapy* restored *Pdlim2* expression in lung tumors and reduced tumor burden; more importantly, co-treatment of nanoPDLIM2 enhanced the efficacy of anti-PD-1 and chemotherapeutic drugs and induced complete remission of all lung cancers in most animals.

Most human lung cancers as well as lung cancers in our animal model have low numbers of TILs and decreased expression of PD-L1 and MHC-I on the cell surface [6, 9], all of which contribute to the resistance to PD-1 blockade therapy. Through inducing immunogenic cell death (ICD) of cancer cells [8], chemotherapy can increase TILs in tumor microenvironment and PD-L1 expression on tumor cells, and thereby synergize with anti-PD-1. However, chemotherapy cannot induce MHC-I expression, this limits further improvement of its synergy with immune therapy for complete cancer remission. Also, tumor cells usually express high levels of survival genes against the tumorcidal effects of chemotherapeutic drugs and of CTLs, including those activated by chemotherapy and unleashed by ICIs.

On the other hand, nanoPDLIM2 induced MHC-I expression and lymphocyte tumor infiltration but did not up-regulate PD-L1. Moreover, nanoPDLIM2 prevented the induction of *Mdr1* and the expression of tumor survival genes, this would further sensitize tumor cells to the cytotoxicity of chemotherapeutic drugs and immune cells. Consistent with these, nanoPDLIM2 improved the efficacy of chemotherapy and PD-1 blockade therapy, and the combination of these three therapies resulted in complete cancer remission in 60% of the animals and dramatic tumor reduction in the remaining mice.

Another important clinical characteristic of *PDLIM2 nanotherapy* is its tumor-specificity and high safety profile. It delivered *Pdlim2*-expression plasmids specifically to lung tumor tissues and increased *Pdlim2* expression. Of note, nanoPDLIM2 showed undetectable toxicity in the animal model, and did not further increase the toxicity of anti-PD-1 and chemotherapeutic drugs. In contrast, although epigenetic drugs (5-aza-dC and MS-275) could restore *PDLIM2* expression in cancer cells with *PDLIM2* epigenetic repression [6, 10-15] and showed better efficacy as a monotherapy or combined with chemotherapeutic drugs or anti-PD-1 than nanoPDLIM2 (Supplementary Figure S4), the epi-drugs caused body weight loss and much worse toxicity when combined with chemotherapy (Supplementary Figure S3). In addition, the therapeutic efficiency of epigenetic drugs depends on *PDLIM2* expression [6]. Although epigenetic therapy can be applicable to 26% lung cancers with *PDLIM2* epigenetic repression, it is not suitable in about 58% of lung cancers harboring *PDLIM2* LOH with copy number losses. NanoPDLIM2, on the other hand, provides a strategy to restore *PDLIM2* expression in all lung cancers with *PDLIM2* repression, regardless of whether it is resulted from promoter hypermethylation or gene deletion.

Conclusions

In summary, the presented data identify genetic deletions as a major mechanism for *PDLIM2* repression in human lung cancers, and *PDLIM2* as a haploinsufficient tumor suppressor particularly important for suppressing lung cancer and therapy resistance. More importantly, these preclinical data demonstrate that combination treatment of nanoPDLIM2, anti-PD-1 and chemotherapeutic drugs induced complete remission of all lung cancers in most animals with high safety profile, suggesting nanoPDLIM2 as a potential strategy to enhance the efficacy of current therapies.

Abbreviations

AC: adenocarcinoma; BFA: brefeldin A; CNV: copy number variation; CTL: cytotoxic T lymphocyte; FACS: fluorescent activated cell sorting; FDA: Food and Drug Administration; IFNγ: interferon-γ; ICD: immunogenic cell death; ICI: immune checkpoint inhibitor; IHC: immunohistochemistry; i.p.: intraperitoneal; i.v.: intravenous; LOH: loss of heterozygosity; Mdr1: multi-drug resistance 1; MHC-I: major histocompatibility complex class I; nanoPDLIM2: nanoparticle-encapsulated *Pdlim2*-expression plasmids; NF-κB: nuclear factor-κB; NIH: National Institutes of Health; ORR: objective response rate; OS: overall survival; PD-1: programmed cell death 1; PD-L1: programmed death ligand 1; PD-L2: programmed death ligand 2; PDLIM2: PDZ-LIM domain-containing protein 2; PEI: polyethylenimine; PFS: progression-free survival; PMA: phorbol 12-myristate 13-acetate; qPCR: quantitative polymerase chain reaction; SEM: standard error of the mean; STAT3: signal transducer and activator of transcription 3; TCGA: The Cancer Genome Atlas; TIL: tumor-infiltrating lymphocyte; WT: wild type.

Acknowledgments

The authors thank Dr. M. J. Grusby (Harvard School of Public Health) and Dr. J. A. Whitsett (University of Cincinnati College of Medicine) for providing PDLIM2$^{-/-}$ and SP-C-rtTA$^{tg/-}$/(tetO)7CMV-Cre$^{tg/tg}$ mice, respectively. The authors also thank Dr. W. Ma and Dr. S. Li (University of Pittsburgh) for their suggestions on the nanoparticle preparation, and Dr. L. H. Rigatti (University of Pittsburgh) for her histological diagnosis of mouse tissues.

Funding

This study was financially supported in part by the NIH National Institute of General Medical Sciences (NIGMS) grant R01 GM144890, National Cancer Institute (NCI) grant R01 CA172090, R21 CA259706, American Cancer Society (ACS) Research Scholar grant RSG-19-166-01-TBG, and American Lung Association (ALA) Lung Cancer Discovery Award 821321.

Availability of data and materials

TCGA lung adenocarcinoma, lung squamous cell carcinoma, and lung cancer data we analyzed were obtained from https://portal.gdc.cancer.gov/projects. All data generated or analyzed during this study are included in this article and its additional files. The Extra data that support the findings of this study are available from the corresponding authors upon reasonable request.

Author contributions

Z.Q. and G.X. conceived and designed the study, led and contributed to all aspects of the analysis, and wrote the manuscript. S.D.S. contributed to the overall experimental design and data analysis and interpretation, provided advice and constructive feedback, and edited the manuscript. F.S. performed and analyzed all the experimental assays. H.Z. contributed to data analysis and edited the manuscript. P.Y. originally identified PDLIM2 LOH in human lung cancers by gene-specific PCR-based LOH analysis. Y.X. contributed to mouse clone maintenance and IHC staining.

Ethics approval and consent to participate

All animal studies were approved by the Institutional Animal Care and Use Committee of the University of Pittsburgh and carried out in accordance with NIH guidelines on animal care.

Consent for publication

Not applicable.

Competing interests

The authors declare that they have no competing interests.

References

[1] Siegel RL, Miller KD, Fuchs HE, Jemal A (2022) Cancer statistics, 2022. *CA Cancer J Clin* **72**, 7-33.

[2] Doroshow DB, Sanmamed MF, Hastings K, Politi K, Rimm DL, Chen L, Melero I, Schalper KA, Herbst RS (2019) Immunotherapy in Non-Small Cell Lung Cancer: Facts and Hopes. *Clin Cancer Res* **25**, 4592-4602.

[3] Zou W, Wolchok JD, Chen L (2016) PD-L1 (B7-H1) and PD-1 pathway blockade for cancer therapy: Mechanisms, response biomarkers, and combinations. *Sci Transl Med* **8**, 328rv324.

[4] Zappasodi R, Merghoub T, Wolchok JD (2018) Emerging Concepts for Immune Checkpoint Blockade-Based Combination Therapies. *Cancer Cell* **34**, 690.

[5] Baxevanos P, Mountzios G (2018) Novel chemotherapy regimens for advanced lung cancer: have we reached a plateau? *Ann Transl Med* **6**, 139.

[6] Sun F, Li L, Yan P, Zhou J, Shapiro SD, Xiao G, Qu Z (2019) Causative role of PDLIM2 epigenetic repression in lung cancer and therapeutic resistance. *Nat Commun* **10**, 5324.

[7] Garassino MC, Gadgeel S, Esteban E, Felip E, Speranza G, Domine M, Hochmair MJ, Powell S, Cheng SY, Bischoff HG, Peled N, Reck M, Hui R, Garon EB, Boyer M, Wei Z, Burke T, Pietanza MC, Rodriguez-Abreu D (2020) Patient-reported outcomes following pembrolizumab or placebo plus pemetrexed and platinum in patients with previously untreated, metastatic, non-squamous non-small-cell lung cancer (KEYNOTE-189): a multicentre, double-blind, randomised, placebo-controlled, phase 3 trial. *Lancet Oncol* **21**, 387-397.

[8] Leonetti A, Wever B, Mazzaschi G, Assaraf YG, Rolfo C, Quaini F, Tiseo M, Giovannetti E (2019) Molecular basis and rationale for combining immune checkpoint inhibitors with chemotherapy in non-small cell lung cancer. *Drug Resist Updat* **46**, 100644.

[9] Sun F, Guo ZS, Gregory AD, Shapiro SD, Xiao G, Qu Z (2020) Dual but not single PD-1 or TIM-3 blockade enhances oncolytic virotherapy in refractory lung cancer. *J Immunother Cancer* **8**.

[10] Guo ZS, Qu Z (2021) PDLIM2: Signaling pathways and functions in cancer suppression and host immunity. *Biochim Biophys Acta Rev Cancer* **1876**, 188630.

[11] Qu Z, Fu J, Yan P, Hu J, Cheng SY, Xiao G (2010) Epigenetic repression of PDZ-LIM domain-containing protein 2: implications for the biology and treatment of breast cancer. *J Biol Chem* **285**, 11786-11792.

[12] Qu Z, Yan P, Fu J, Jiang J, Grusby MJ, Smithgall TE, Xiao G (2010) DNA methylation-dependent repression of PDZ-LIM domain-containing protein 2 in colon cancer and its role as a potential therapeutic target. *Cancer Res* **70**, 1766-1772.

[13] Sun F, Xiao Y, Qu Z (2015) Oncovirus Kaposi sarcoma herpesvirus (KSHV) represses tumor suppressor PDLIM2 to persistently activate nuclear factor kappaB (NF-kappaB) and STAT3 transcription factors for tumorigenesis and tumor maintenance. *J Biol Chem* **290**, 7362-7368.

[14] Yan P, Qu Z, Ishikawa C, Mori N, Xiao G (2009) Human T-cell leukemia virus type I-mediated repression of PDZ-LIM domain-containing protein 2 involves DNA methylation but independent of the viral oncoprotein tax. *Neoplasia* **11**, 1036-1041.

[15] Vanoirbeek E, Eelen G, Verlinden L, Carmeliet G, Mathieu C, Bouillon R, O'Connor R, Xiao G, Verstuyf A (2014) PDLIM2 expression is driven by vitamin D and is involved in the pro-adhesion, and anti-migration and -invasion activity of vitamin D. *Oncogene* **33**, 1904-1911.

[16] Yan P, Fu J, Qu Z, Li S, Tanaka T, Grusby MJ, Xiao G (2009) PDLIM2 suppresses human T-cell leukemia virus type I Tax-mediated tumorigenesis by targeting Tax into the nuclear matrix for proteasomal degradation. *Blood* **113**, 4370-4380.

[17] Fu J, Yan P, Li S, Qu Z, Xiao G (2010) Molecular determinants of PDLIM2 in suppressing HTLV-I Tax-mediated tumorigenesis. *Oncogene* **29**, 6499-6507.

[18] Torrado M, Senatorov VV, Trivedi R, Fariss RN, Tomarev SI (2004) Pdlim2, a novel PDZ-LIM domain protein, interacts with alpha-actinins and filamin A. *Invest Ophthalmol Vis Sci* **45**, 3955-3963.

[19] Tanaka T, Soriano MA, Grusby MJ (2005) SLIM is a nuclear ubiquitin E3 ligase that negatively regulates STAT signaling. *Immunity* **22**, 729-736.

[20] Loughran G, Healy NC, Kiely PA, Huigsloot M, Kedersha NL, O'Connor R (2005) Mystique is a new insulin-like growth factor-I-regulated PDZ-LIM domain protein that promotes cell attachment and migration and suppresses Anchorage-independent growth. *Mol Biol Cell* **16**, 1811-1822.

[21] Tanaka T, Grusby MJ, Kaisho T (2007) PDLIM2-mediated termination of transcription factor NF-kappaB activation by intranuclear sequestration and degradation of the p65 subunit. *Nat Immunol* **8**, 584-591.

[22] Qu Z, Fu J, Ma H, Zhou J, Jin M, Mapara MY, Grusby MJ, Xiao G (2012) PDLIM2 restricts Th1 and Th17 differentiation and prevents autoimmune disease. *Cell Biosci* **2**, 23.

[23] Zhou J, Qu Z, Yan S, Sun F, Whitsett JA, Shapiro SD, Xiao G (2015) Differential roles of STAT3 in the initiation and growth of lung cancer. *Oncogene* **34**, 3804-3814.

[24] Qu Z, Sun F, Zhou J, Li L, Shapiro SD, Xiao G (2015) Interleukin-6 Prevents the Initiation but Enhances the Progression of Lung Cancer. *Cancer Res* **75**, 3209-3215.

[25] Steinbrecher KA, Harmel-Laws E, Sitcheran R, Baldwin AS (2008) Loss of epithelial RelA results in deregulated intestinal proliferative/apoptotic homeostasis and susceptibility to inflammation. *J Immunol* **180**, 2588-2599.

[26] Yu H, Pardoll D, Jove R (2009) STATs in cancer inflammation and immunity: a leading role for STAT3. *Nat Rev Cancer* **9**, 798-809.

[27] Xiao G, Fu J (2011) NF-kappaB and cancer: a paradigm of Yin-Yang. *Am J Cancer Res* **1**, 192-221.

[28] Li L, Sun F, Han L, Liu X, Xiao Y, Gregory AD, Shapiro SD, Xiao G, Qu Z (2021) PDLIM2 repression by ROS in alveolar macrophages promotes lung tumorigenesis. *JCI Insight* **6**.

[29] Sun F, Li L, Xiao Y, Gregory AD, Shapiro SD, Xiao G, Qu Z (2021) Alveolar Macrophages Inherently Express Programmed Death-1 Ligand 1 for Optimal Protective Immunity and Tolerance. *J Immunol* **207**, 110-114.

[30] Wistuba, II, Behrens C, Virmani AK, Milchgrub S, Syed S, Lam S, Mackay B, Minna JD, Gazdar AF (1999) Allelic losses at chromosome 8p21-23 are early and frequent events in the pathogenesis of lung cancer. *Cancer Res* **59**, 1973-1979.

[31] Kang J (2015) Genomic alterations on 8p21-p23 are the most frequent genetic events in stage I squamous cell carcinoma of the lung. *Exp Ther Med* **9**, 345-350.

[32] Macartney-Coxson DP, Hood KA, Shi HJ, Ward T, Wiles A, O'Connor R, Hall DA, Lea RA, Royds JA, Stubbs RS, Rooker S (2008) Metastatic susceptibility locus, an 8p hot-spot for tumour progression disrupted in colorectal liver metastases: 13 candidate genes examined at the DNA, mRNA and protein level. *BMC Cancer* **8**, 187.

[33] Swalwell JI, Vocke CD, Yang Y, Walker JR, Grouse L, Myers SH, Gillespie JW, Bostwick DG, Duray PH, Linehan WM, Emmert-Buck MR (2002) Determination of a minimal deletion interval on chromosome band 8p21 in sporadic prostate cancer. *Genes Chromosomes Cancer* **33**, 201-205.

[34] Wurster KD, Hummel F, Richter J, Giefing M, Hartmann S, Hansmann ML, Kreher S, Kochert K, Krappmann D, Klapper W, Hummel M, Wenzel SS, Lenz G, Janz M, Dorken B, Siebert R, Mathas S (2017) Inactivation of the putative ubiquitin-E3 ligase PDLIM2 in classical Hodgkin and anaplastic large cell lymphoma. *Leukemia* **31**, 602-613.

[35] Matouk I, Raveh E, Ohana P, Lail RA, Gershtain E, Gilon M, De Groot N, Czerniak A, Hochberg A (2013) The increasing complexity of the oncofetal h19 gene locus: functional dissection and therapeutic intervention. *Int J Mol Sci* **14**, 4298-4316.

[36] Buscail L, Bournet B, Vernejoul F, Cambois G, Lulka H, Hanoun N, Dufresne M, Meulle A, Vignolle-Vidoni A, Ligat L, Saint-Laurent N, Pont F, Dejean S, Gayral M, Martins F, Torrisani J, Barbey O, Gross F, Guimbaud R, Otal P, Lopez F, Tiraby G, Cordelier P (2015) First-in-man

phase 1 clinical trial of gene therapy for advanced pancreatic cancer: safety, biodistribution, and preliminary clinical findings. *Mol Ther* **23**, 779-789.

[37] Nyamay'Antu A, Dumont M, Kedinger V, Erbacher p (2019) Non-Viral Vector Mediated Gene Delivery: the Outsider to Watch Out For in Gene Therapy. *Cell & Gene Therapy Insights* **5**, 7.

[38] Bonnet ME, Erbacher P, Bolcato-Bellemin AL (2008) Systemic delivery of DNA or siRNA mediated by linear polyethylenimine (L-PEI) does not induce an inflammatory response. *Pharm Res* **25**, 2972-2982.

[39] Yang J, Hendricks W, Liu G, McCaffery JM, Kinzler KW, Huso DL, Vogelstein B, Zhou S (2013) A nanoparticle formulation that selectively transfects metastatic tumors in mice. *Proc Natl Acad Sci U S A* **110**, 14717-14722.

[40] Kellar A, Egan C, Morris D (2015) Preclinical Murine Models for Lung Cancer: Clinical Trial Applications. *Biomed Res Int* **2015**, 621324.

[41] Zhou J, Qu Z, Sun F, Han L, Li L, Yan S, Stabile LP, Chen LF, Siegfried JM, Xiao G (2017) Myeloid STAT3 Promotes Lung Tumorigenesis by Transforming Tumor Immunosurveillance into Tumor-Promoting Inflammation. *Cancer Immunol Res* **5**, 257-268.

[42] Li L, Han L, Sun F, Zhou J, Ohaegbulam KC, Tang X, Zang X, Steinbrecher KA, Qu Z, Xiao G (2018) NF-kappaB RelA renders tumor-associated macrophages resistant to and capable of directly suppressing CD8(+) T cells for tumor promotion. *Oncoimmunology* **7**, e1435250.

[43] Sun F, Qu Z, Xiao Y, Zhou J, Burns TF, Stabile LP, Siegfried JM, Xiao G (2016) NF-kappaB1 p105 suppresses lung tumorigenesis through the Tpl2 kinase but independently of its NF-kappaB function. *Oncogene* **35**, 2299-2310.

[44] Hecht SS (2002) Cigarette smoking and lung cancer: chemical mechanisms and approaches to prevention. *Lancet Oncol* **3**, 461-469.

[45] Commisso C, Davidson SM, Soydaner-Azeloglu RG, Parker SJ, Kamphorst JJ, Hackett S, Grabocka E, Nofal M, Drebin JA, Thompson CB, Rabinowitz JD, Metallo CM, Vander Heiden MG, Bar-Sagi D (2013) Macropinocytosis of protein is an amino acid supply route in Ras-transformed cells. *Nature* **497**, 633-637.

[46] Huang JL, Jiang G, Song QX, Gu X, Hu M, Wang XL, Song HH, Chen LP, Lin YY, Jiang D, Chen J, Feng JF, Qiu YM, Jiang JY, Jiang XG, Chen HZ, Gao XL (2017) Lipoprotein-biomimetic nanostructure enables efficient targeting delivery of siRNA to Ras-activated glioblastoma cells via macropinocytosis. *Nat Commun* **8**, 15144.

[47] Shi J, Kantoff PW, Wooster R, Farokhzad OC (2017) Cancer nanomedicine: progress, challenges and opportunities. *Nat Rev Cancer* **17**, 20-37.

Figure legends

Fig 1. *PDLIM2* repression in human lung cancers involves both epigenetic alteration and genetic deletion, and *PDLIM2* genetic deletion in mice leads to development of spontaneous tumors, majorly lung tumors. (A) TCGA data showing *PDLIM2* repression in over 90% of lung cancers if using 50% of the expression level in normal lung tissues as the cut-off (NL, n = 110; Tumor, n = 1019). (B) TCGA data showing *PDLIM2* promoter hypermethylation and expression repression (dashed box) in over 70% of lung cancers when using 125% of the methylation level in normal lung tissues as the cut-off (n = 827). (C) TCGA data showing positive associations between *PDLIM2* expression and its gene copy numbers as well as PDLIM2 genetic deletion and expression repression (dashed box) in about 58% of lung cancers using the copy number variation of -0.1 as the cut-off (n = 1010). (D) TCGA data showing simultaneous promoter hypermethylation and genomic deletion of *PDLIM2* (dashed box) in about 44% of lung cancers (n = 816). (E) Microsatellite-PCR showing *pdlim2* loss in human lung cancers (n = 21). (F) qPCR showing *PDLIM2* loss in human lung cancer cell lines with known copy number of the *PDLIM2* gene (n = 25). (G) Kaplan-Meier tumor-free survival curve showing increased spontaneous tumors in *Pdlim2*$^{-/-}$ and *Pdlim2*$^{+/-}$ mice compared to WT mice. Gehan-Breslow-Wilcoxon test was performed. $*p < 0.05$. (H) Percentage of tumor types spontaneously developed in *Pdlim2*$^{+/-}$ mice, and 51% of tumors occurred in the lung.

Figure 2. Systemic administration of PDLIM2 plasmid nanoparticles shows efficacy in mouse model of refractory lung cancer. (A) Schedule of lung cancer induction and treatment. (B) Intravenous administration of PDLIM2 plasmid nanoparticles reduced lung tumors in mouse urethane lung tumor model ($n \geq 6$). Nanoparticles carrying an empty vector plasmid (Vec) that was employed to express PDLIM2 were used as a control. (C) IHC staining showing decreased nuclear expression of Stat 3 and Rela in lung tumors by PDLIM2 nanotherapy (n = 6). (D) IHC staining showing decreased Bcl-xl and increased cleaved caspase -3 in lung tumors by PDLIM2 nanotherapy (n = 6). (E) IHC staining showing decreased Cyclin D1 and proliferation (Brdu) in lung tumors by PDLIM2 nanotherapy (n = 6). Scale bar

in (C-E), 20 μm. Student's *t* test was performed (two tailed, unpaired) and data represent means ± SEM in (B-E). $^{**}p < 0.01$; ns, not statistically significant.

Figure 3 PDLIM2 nanotherapy shows high tumor specificity and low toxicity. (A) IHC staining showing high Pdlim2 re-expression in lung tumors after PDLIM2 nanotherapy. (B) PCR and IB assays showing lung tumor-specific plasmids delivery and PDLIM2 expression by PDLIM2 nanotherapy (n = 3). (C) IHC staining showing comparable expression of PDLIM2 in the indicated tissues of mice treated with PDLIM2 expression plasmid or empty vector plasmid nanoparticles. (D) No significant changes in animal body weight by PDLIM2nanoparticles (n = 5). (E) H&E staining showing no noticeable changes in major organs by PDLIM2nanoparticles nanotherapy. Scale bar: (A and C) 20 μm; (E) 50 μm.

Figure 4 PDLIM2 nanotherapy renders lung cancers more vulnerable to chemotherapy. (A) Synergy of PDLIM2 nanotherapy and chemotherapeutic drugs (carboplatin and paclitaxel) to reduce lung tumors in lung tumor models induced by urethane ($n \geq 5$). (B) IHC staining showing effects on lung tumor cell apoptosis by PDLIM2nanoparticle, chemo-drugs, and their combination (n = 6). (C) IHC staining showing increase in nuclear Rela by chemotherapy and its inhibition by PDLIM2nanoparticles (n = 6). (D) IHC staining showing MDR1 induction by chemotherapy and its blockage by PDLIM2 nanotherapy (n = 6). Scale bar in (B-D), 20 μm. Student's *t* test was performed (two tailed, unpaired) and data represent means ± SEM. $^{*}p < 0.05$; $^{**}p < 0.01$; ns, not statistically significant.

Figure 5 PDLIM2 nanotherapy increases the efficacy of PD-1 blockade immunotherapy. (A) IHC staining showing increased TILs in lung tumors by PDLIM2nanoparticles (n = 6). (B) FACS showing increased MHC-I expression in lung tumor cells by PDLIM2 nanotherapy (n = 4). (C) Enhancing effects of PDLIM2nanoparticles on PD-1 immunotherapy in lung tumors induced by urethane ($n \geq 5$). (D) IHC staining showing increased TILs by PDLIM2 nanotherapy in the context of immunotherapy (n = 6). (E)

FACS showing increased activation of $CD8^+$ T cells by PDLIM2 nanotherapy in the context of immunotherapy (n = 3). (F) IHC staining showing increased lung tumor cell apoptosis by PDLIM2 nanotherapy, immunotherapy, and further increase by their combination (n = 6). Scale bar in (A, D, F), 20 μm. Student's *t* test was performed (two tailed, unpaired) and data represent means ± SEM. $^{**}p < 0.01$; ns, not statistically significant.

Figure 6 Combination of PDLIM2 nanotherapy, chemotherapy and immunotherapy shows enhanced efficacy in lung cancer treatment. (A) IHC staining showing PD-L1 induction by chemotherapy but not by PDLIM2 nanotherapy. (B) Schedule of lung cancer induction and treatment. (C) Urethane-induced lung tumors were more resistant to chemo and αPD-1 combination therapy in mice with Pdlim2 specifically deleted in lung epithelial cells (ΔSPC) ($n \geq 4$). (D) IHC staining showing no MHC-I induction by chemotherapy, PD-1 immunotherapy or their combination (n = 6). (E) Tumor examination showing complete remission of all lung tumors in 60% of mice by combination of the three therapies ($n \geq 5$). (F) IHC staining showing increased TILs by PDLIM2 nanotherapy in mice treated with anti-PD-1 and chemotherapeutic drugs (n = 6). (G) FACS analysis showing increased lung $CD8^+$ T-cell activation by PDLIM2 nanotherapy in mice treated with anti-PD-1 and chemotherapeutic drugs (n = 5). (H) No significant effect of PDLIM2 nanotherapy on the body weight of mice treated with anti-PD-1 and chemotherapeutic drugs (n = 5). Scale bar in (A and F), 20 μm. Student's *t* test was performed (two tailed, unpaired) and data represent means ± SEM in (**c**-**g**). $^{*}p < 0.05$; $^{**}p < 0.01$; ns, not statistically significant.

Figure 1

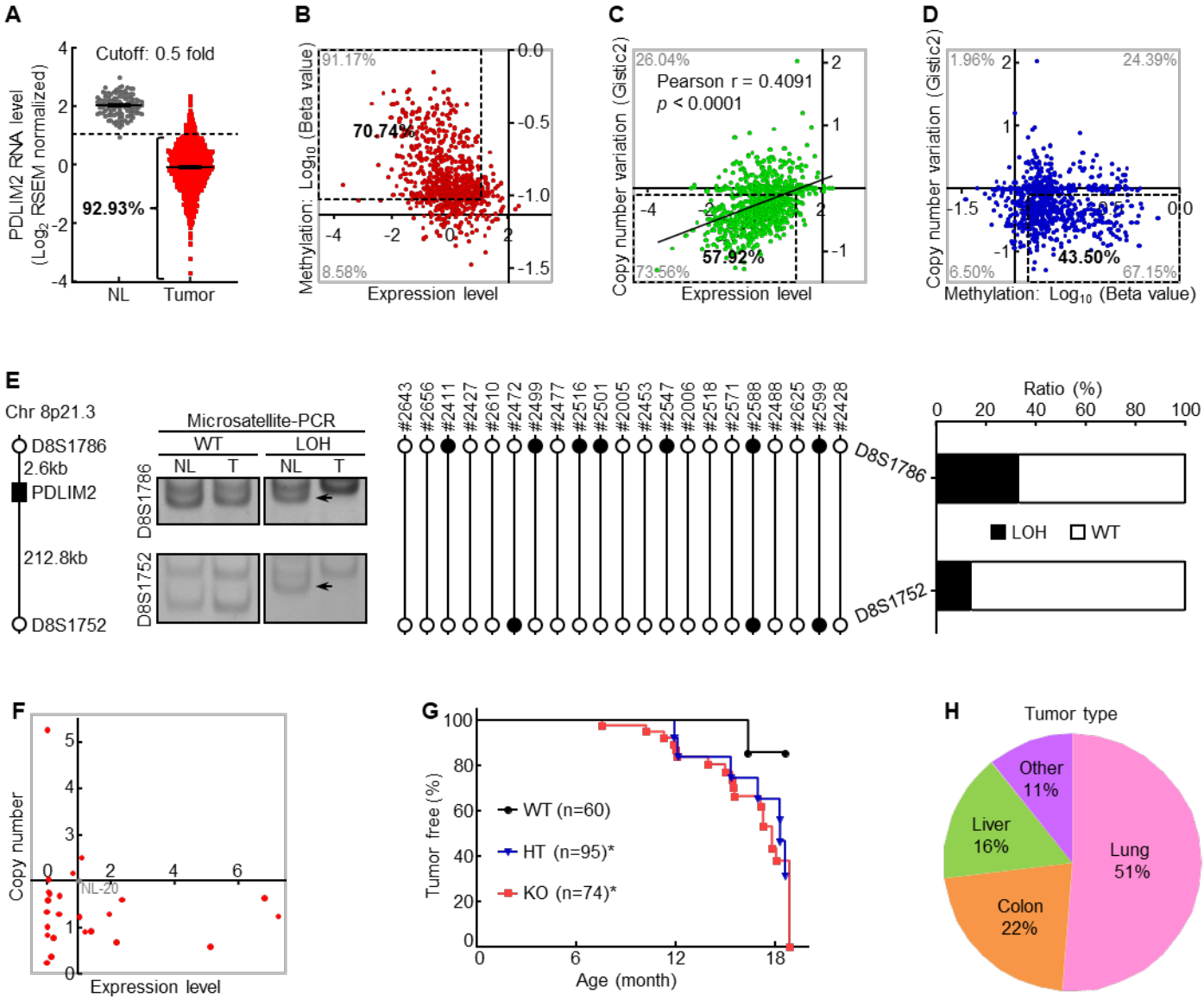
A
Cutoff: 0.5 fold
PDLIM2 RNA level
(Log2 RSEM normalized)
92.93%
NL
Tumor
B
91.17%
70.74%
8.58%
Methylation: Log10 (Beta value)
Expression level
C
26.04%
Pearson r = 0.4091
p < 0.0001
57.92%
73.56%
Copy number variation (Gistic2)
Expression level
D
1.96%
24.39%
43.50%
6.50%
67.15%
Copy number variation (Gistic2)
Methylation: Log10 (Beta value)
E
Chr 8p21.3
D8S1786
2.6kb
PDLIM2
212.8kb
D8S1752
Microsatellite-PCR
WT
LOH
NL
T
D8S1786
D8S1752
#2643
#2656
#2411
#2427
#2610
#2472
#2499
#2477
#2516
#2501
#2005
#2453
#2547
#2006
#2518
#2571
#2588
#2488
#2625
#2599
#2428
Ratio (%)
LOH
WT
F
Copy number
NL-20
Expression level
G
WT (n=60)
HT (n=95)*
KO (n=74)*
Tumor free (%)
Age (month)
H
Tumor type
Other
11%
Liver
16%
Lung
51%
Colon
22%

Figure 2

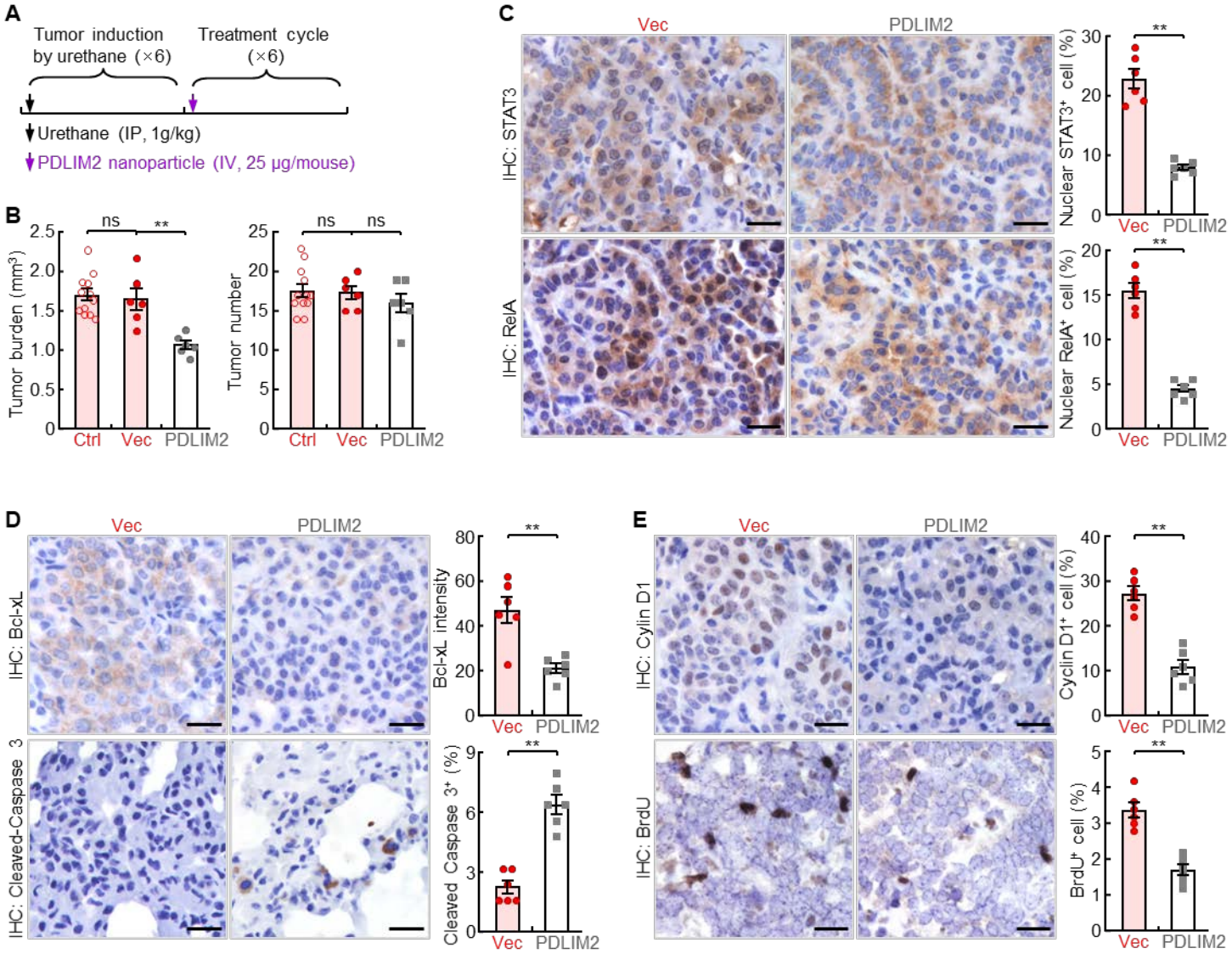
A
Tumor induction by urethane (×6)
Treatment cycle (×6)
Urethane (IP, 1g/kg)
PDLIM2 nanoparticle (IV, 25 μg/mouse)
B
Tumor burden (mm³)
Tumor number
ns
**
Ctrl
Vec
PDLIM2
C
Vec
PDLIM2
IHC: STAT3
IHC: RelA
Nuclear STAT3⁺ cell (%)
Nuclear RelA⁺ cell (%)
D
IHC: Bcl-xL
IHC: Cleaved-Caspase 3
Bcl-xL intensity
Cleaved Caspase 3⁺ (%)
E
IHC: Cylin D1
IHC: BrdU
Cyclin D1⁺ cell (%)
BrdU⁺ cell (%)

Figure 3

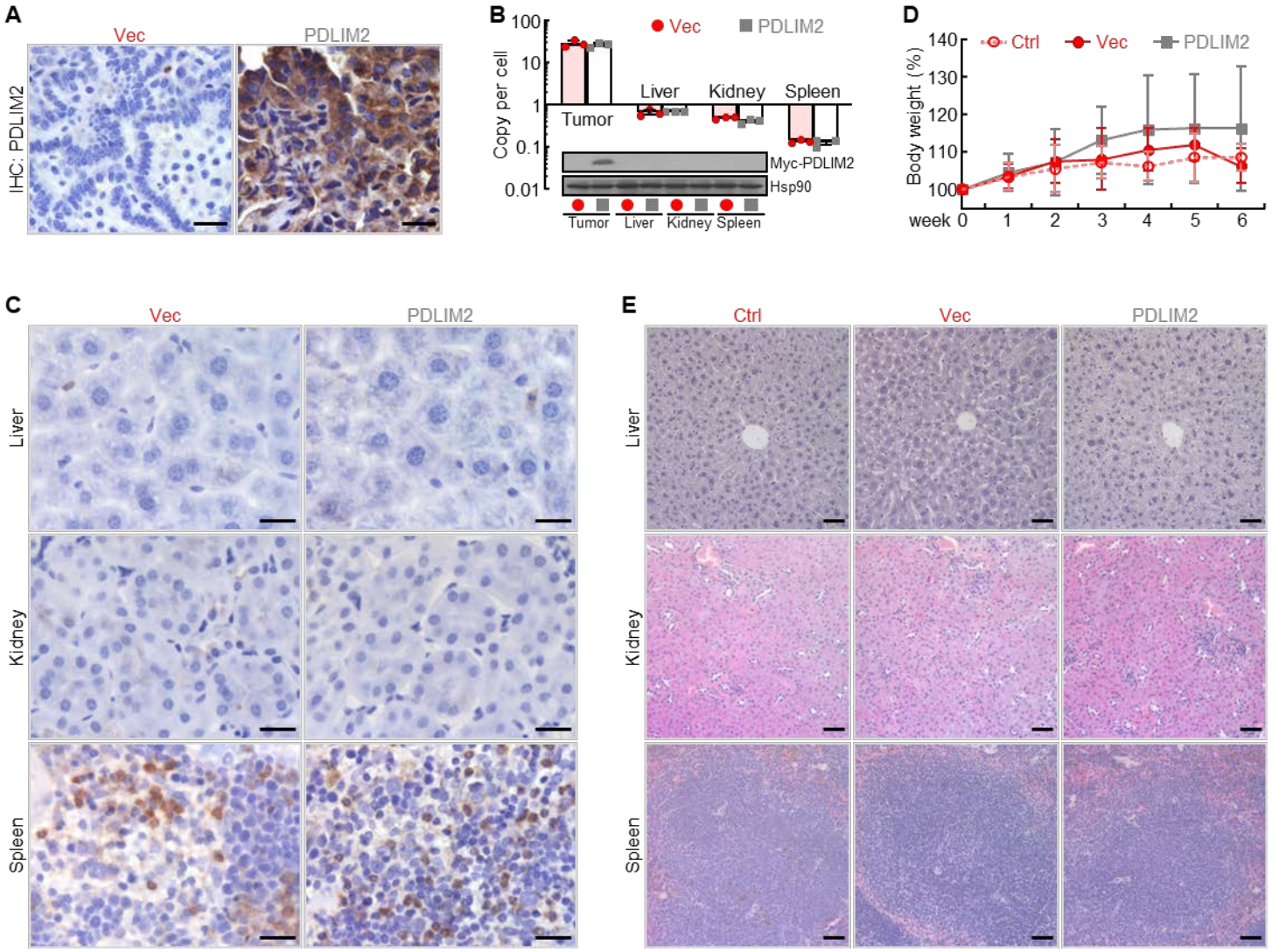
A
Vec
PDLIM2
IHC: PDLIM2
B
Vec
PDLIM2
Copy per cell
100
10
1
0.1
0.01
Tumor
Liver
Kidney
Spleen
Myc-PDLIM2
Hsp90
Tumor
Liver
Kidney
Spleen
D
Ctrl
Vec
PDLIM2
Body weight (%)
140
130
120
110
100
week 0
1
2
3
4
5
6
C
Vec
PDLIM2
Liver
Kidney
Spleen
E
Ctrl
Vec
PDLIM2
Liver
Kidney
Spleen

Figure 4

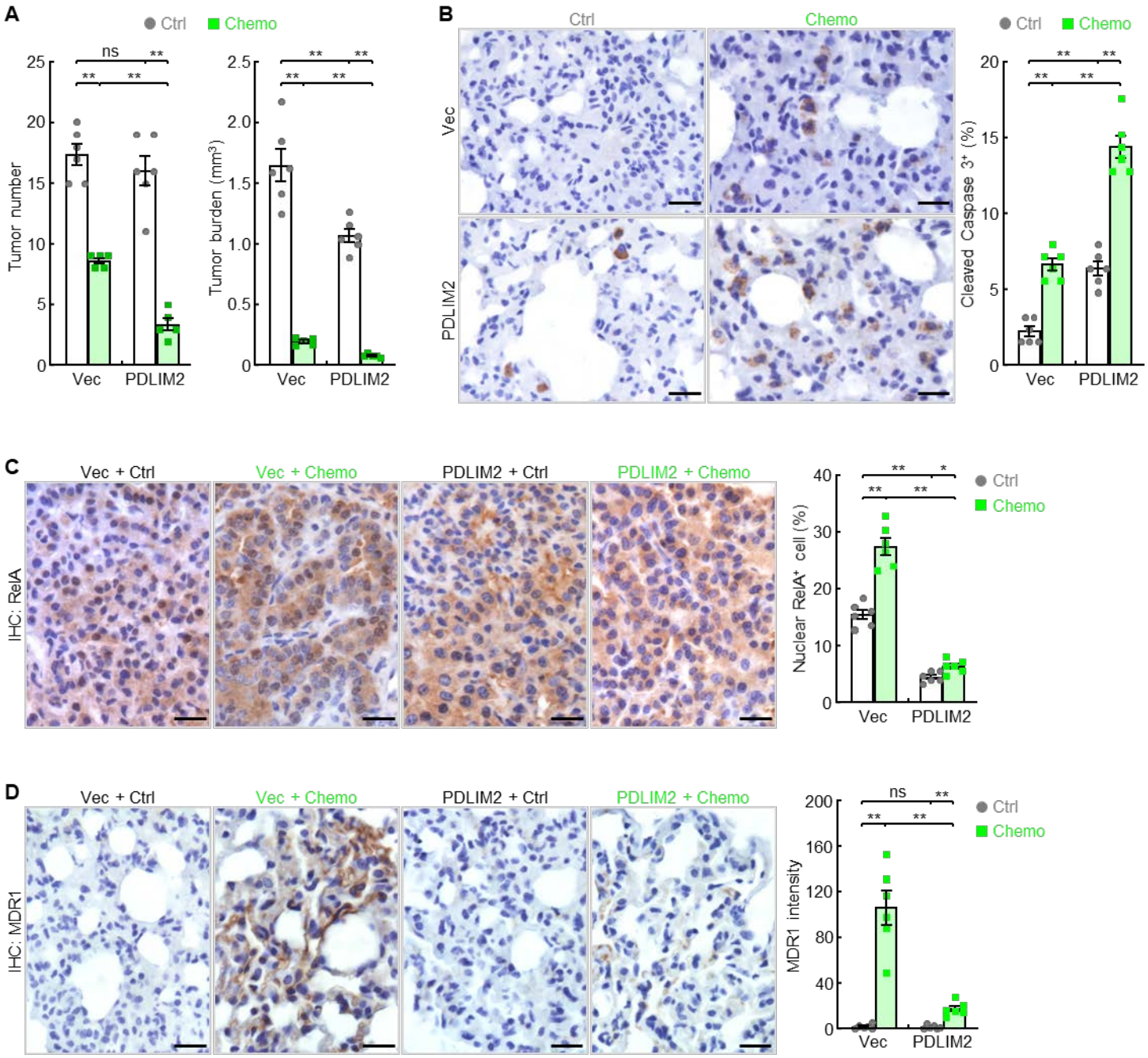
A
Ctrl
Chemo
Tumor number
Tumor burden (mm3)
Vec
PDLIM2
ns
**
B
Ctrl
Chemo
Vec
PDLIM2
Cleaved Caspase 3+ (%)
C
Vec + Ctrl
Vec + Chemo
PDLIM2 + Ctrl
PDLIM2 + Chemo
IHC: RelA
Nuclear RelA+ cell (%)
*
D
IHC: MDR1
MDR1 intensity

Figure 5

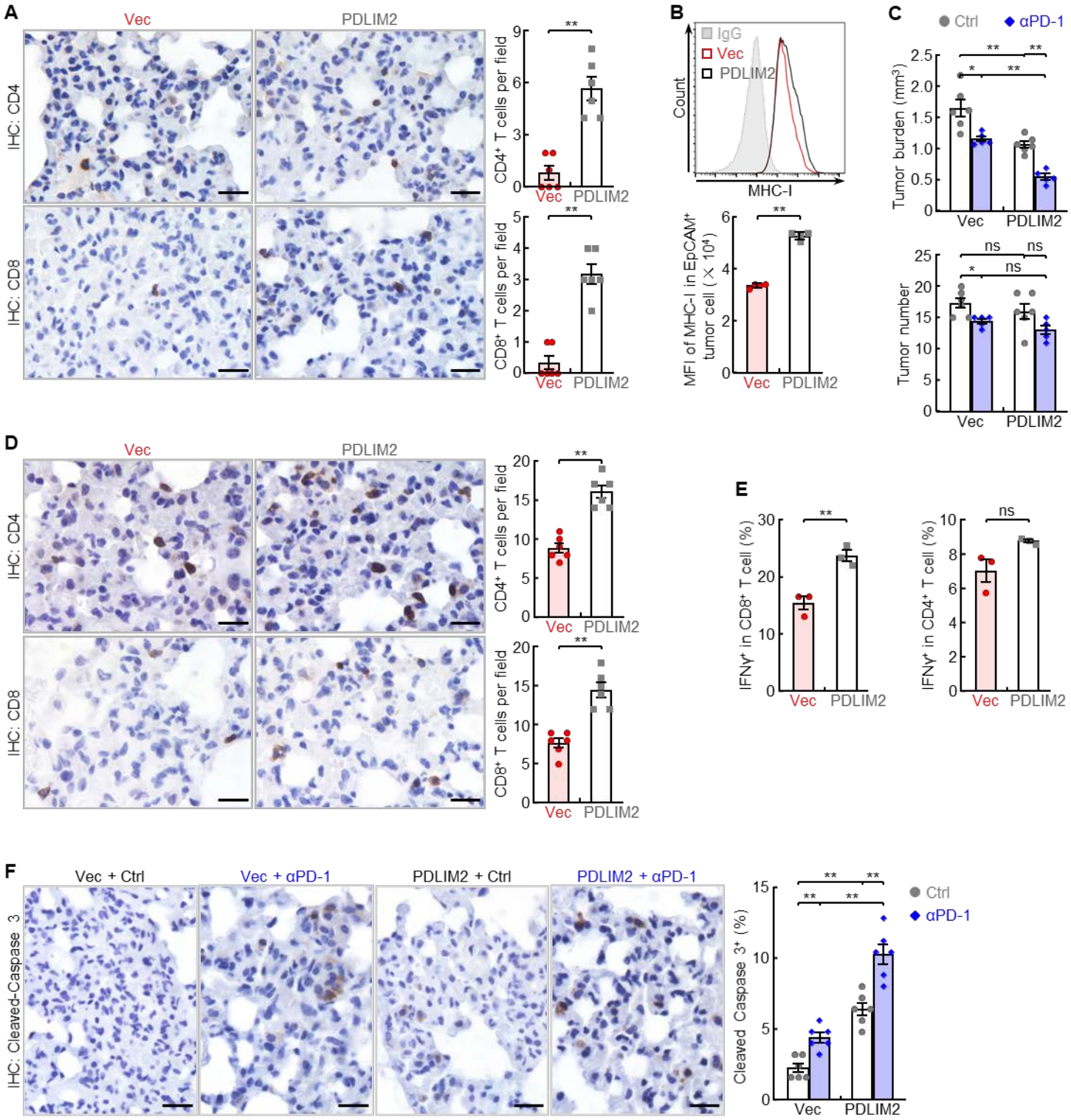
A
Vec
PDLIM2
IHC: CD4
IHC: CD8
CD4⁺ T cells per field
CD8⁺ T cells per field
B
IgG
Vec
PDLIM2
Count
MHC-I
MFI of MHC-I in EpCAM⁺ tumor cell (× 10⁴)
C
Ctrl
αPD-1
Tumor burden (mm³)
Tumor number
ns
D
E
IFNγ⁺ in CD8⁺ T cell (%)
IFNγ⁺ in CD4⁺ T cell (%)
F
Vec + Ctrl
Vec + αPD-1
PDLIM2 + Ctrl
PDLIM2 + αPD-1
IHC: Cleaved-Caspase 3
Cleaved Caspase 3⁺ (%)

Figure 6

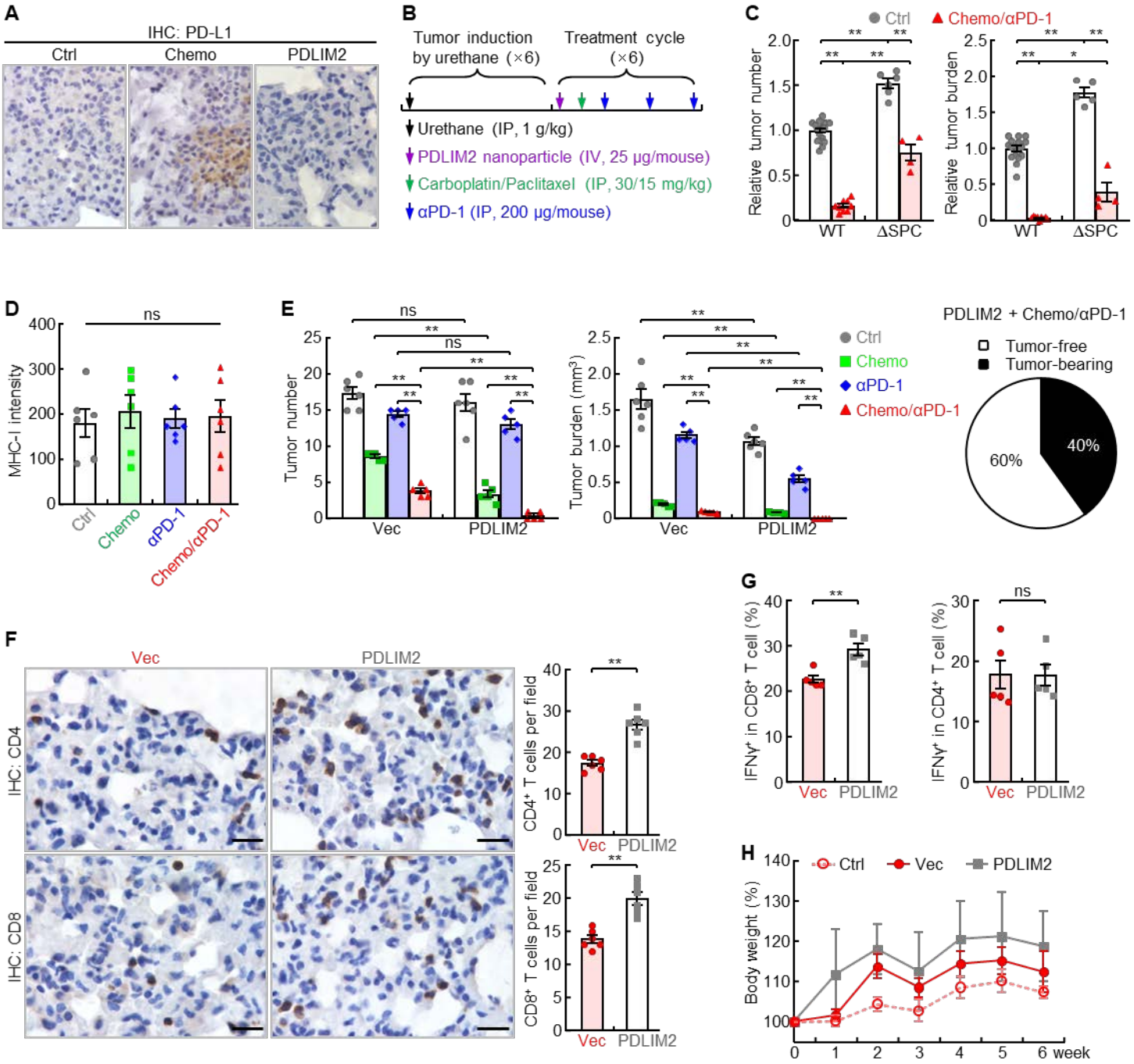
A
IHC: PD-L1
Ctrl
Chemo
PDLIM2
B
Tumor induction by urethane (×6)
Treatment cycle (×6)
Urethane (IP, 1 g/kg)
PDLIM2 nanoparticle (IV, 25 μg/mouse)
Carboplatin/Paclitaxel (IP, 30/15 mg/kg)
αPD-1 (IP, 200 μg/mouse)
C
Ctrl
Chemo/αPD-1
Relative tumor number
Relative tumor burden
WT
ΔSPC
D
MHC-I intensity
ns
Ctrl
Chemo
αPD-1
Chemo/αPD-1
E
Tumor number
Tumor burden (mm³)
Vec
PDLIM2
Ctrl
Chemo
αPD-1
Chemo/αPD-1
PDLIM2 + Chemo/αPD-1
Tumor-free
Tumor-bearing
60%
40%
F
Vec
PDLIM2
IHC: CD4
IHC: CD8
CD4⁺ T cells per field
CD8⁺ T cells per field
G
IFNγ⁺ in CD8⁺ T cell (%)
IFNγ⁺ in CD4⁺ T cell (%)
H
Ctrl
Vec
PDLIM2
Body weight (%)
week

651

Supplemental Table 1. Antibodies Used

Antibody	Company	Cat. No.	Dose	Usage
Anti-PDLIM2	Everest Biotech, Ramona, CA, USA	EB11878	1:400	IHC
Anti-Cleaved Caspase 3	Cell Signaling Technology, Danvers, MA, USA	9661	1:200	IHC
Anti-Bcl-xL	Cell Signaling Technology, Danvers, MA, USA	2764	1:2400	IHC
Anti-Cyclin D1	Santa Cruz Biotechnology, Dallas, TX, USA	sc-450	1:200	IHC
Anti-BrdU	Sigma-Aldrich, St. Louis, MO, USA	B2531	1:500	IHC
Anti-RelA	Cell Signaling Technology, Danvers, MA, USA	8242	1:500	IHC
Anti-STAT3	Cell Signaling Technology, Danvers, MA, USA	4904	1:1000	IHC
Anti-MDR1	Cell Signaling Technology, Danvers, MA, USA	13978	1:800	IHC
Anti-CD4	Abcam, Cambridge, MA, USA	ab183685	1:1000	IHC
Anti-CD8	Abcam, Cambridge, MA, USA	ab209775	1:1000	IHC
Anti-PD-L1	Cell Signaling Technology, Danvers, MA, USA	64988	1:200	IHC
Anti-MHC-I	Abcam, Cambridge, MA, USA	ab15681	1:200	IHC
Anti-mouse IgG Biotinylated	Vector Laboratories, Burlingame, CA, USA	BMK-2202	1:200	IHC
Goat anti-rat IgG Biotinylated	Vector Laboratories, Burlingame, CA, USA	BA9401	1:100	IHC
Rabbit anti-goat IgG Biotinylated	Santa Cruz Biotechnology, Dallas, TX, USA	sc-2774	1:200	IHC
Goat anti-rabbit IgG Biotinylated	Dako, Carpinteria, CA, USA	E0432	1:200	IHC
Anti-Hsp90	Santa Cruz Biotechnology, Dallas, TX, USA	sc-13119	1:1000	WB
Anti-c-Myc	Santa Cruz Biotechnology, Dallas, TX, USA	sc-40	1:1000	WB
Anti-CD16/CD32	eBioscience, San Diego, CA, USA	14-0161-85	1.0 µl per sample	FACS
Anti-CD45 FITC	Biolegend, San Diego, CA, USA	103107	0.5 µl per sample	FACS
Anti-EpCAM PE	eBioscience, San Diego, CA, USA	12-5791-82	0.625 µl per sample	FACS
Anti-MHC-I APC	eBioscience, San Diego, CA, USA	17-5998-82	1.25 µl per sample	FACS
Anti-CD3 PE	eBioscience, San Diego, CA, USA	12-0031-83	2.5 µl per sample	FACS
Anti-CD4 PE-Cy7	eBioscience, San Diego, CA, USA	25-0042-82	1.25 µl per sample	FACS
Anti-CD8a APC	eBioscience, San Diego, CA, USA	17-0081-83	0.625 µl per sample	FACS
Anti-IFNγ FITC	eBioscience, San Diego, CA, USA	11-7311-82	1 µl per sample	FACS
Anti-PD-1	BioXcell, West Lebanon, NH, USA	BE0273	200 µg/mouse/time	*in vivo* blockade

652

Supplemental Table 2. Primers Used

Gene	Species	Accession number	Forward (5' to 3')	Reverse (5' to 3')	Usage
D8S1786	human		CGAAAGATTGAGACCCCAT	GTTTCCACACCGAAGCC	Microsatellite PCR
D8S1752	human		TCCTGGATCAGGCAGAAA	TCAGAGTTGGGTGAGCGA	Microsatellite PCR
line-1	human	M80343.1	AAAGCCGCTCAACTACATGG	TGCTTTGAATGCGTCCCAGAG	RT-PCR
pdlim2	human	NG_030435.1	CAAAGCCAAGGACGCTGACC	GCTCTGGCGGATCTTGCTCT	RT-PCR
pdlim2	mouse	Mutant primer	GCTACCCGTGATATTGCTGAAGAG		Genotyping PCR
		WT primer	GTCTTCTCTTCCTCAGGCATGGCG		
		Common primer	GCCAACATTGCCCCAGAAGACTCC		
Amp-R	Plasmid		AACTTTATCCGCCTCCAT	GAAGCCATACCAAACGAC	Plasmid detection
Lyz2	mouse	NC_000076.6	AGCAGGCATGCTTTCTCTAGTC	GCGATTAGCTGGAGCCATCA	

Supplemental Table 3. PDLIM2 RNA level and copy number in human lung cancer cell lines

	PDLIM2 gene	
	Relative RNA level	Copy number
NL-20	1.000	2.000
CALU-6	0.010	1.021
H727	0.020	1.590
H460	0.001	1.341
H2122	0.042	2.038
H23	0.128	0.376
H358	7.260	1.244
SKLU-1	0.390	1.685
SW1573	0.010	0.842
CALU-1	1.950	1.293
128-88T	0.049	1.767
H1299	0.003	0.243
273T	0.815	2.172
H827	1.017	1.237
H1650	2.168	0.679
H3255	5.118	0.587
343T	1.365	0.919
CALU-3	0.377	1.290
H1435	1.198	0.915
H1793	6.833	1.637
H596	0.195	0.782
H838	0.080	1.740
H1838	2.360	1.603
A549	0.010	5.265
H1975	1.086	2.507

Supplement Figure S1

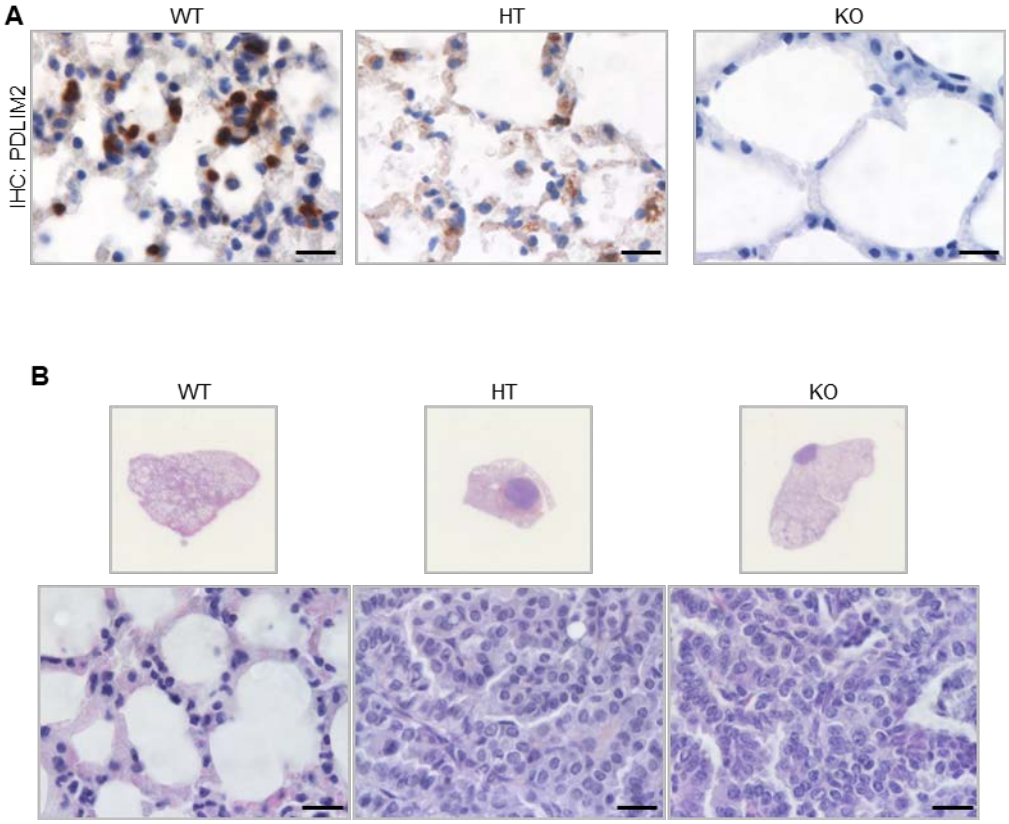

Figure S1. Mice with PDLIM2 deletion develop spontaneous tumors, majorly lung tumors. A, IHC assays showing decreased and complete loss of PDLIM2 protein expression in the lungs of PDLIM2+/- and PDLIM2-/- mice, respectively. Scale bar, 20 µm. B, H&E staining of the lung tissues showing spontaneous lung tumors in PDLIM2+/- and PDLIM2-/- mice. Scale bar, 20 µm.

Supplement Figure S2

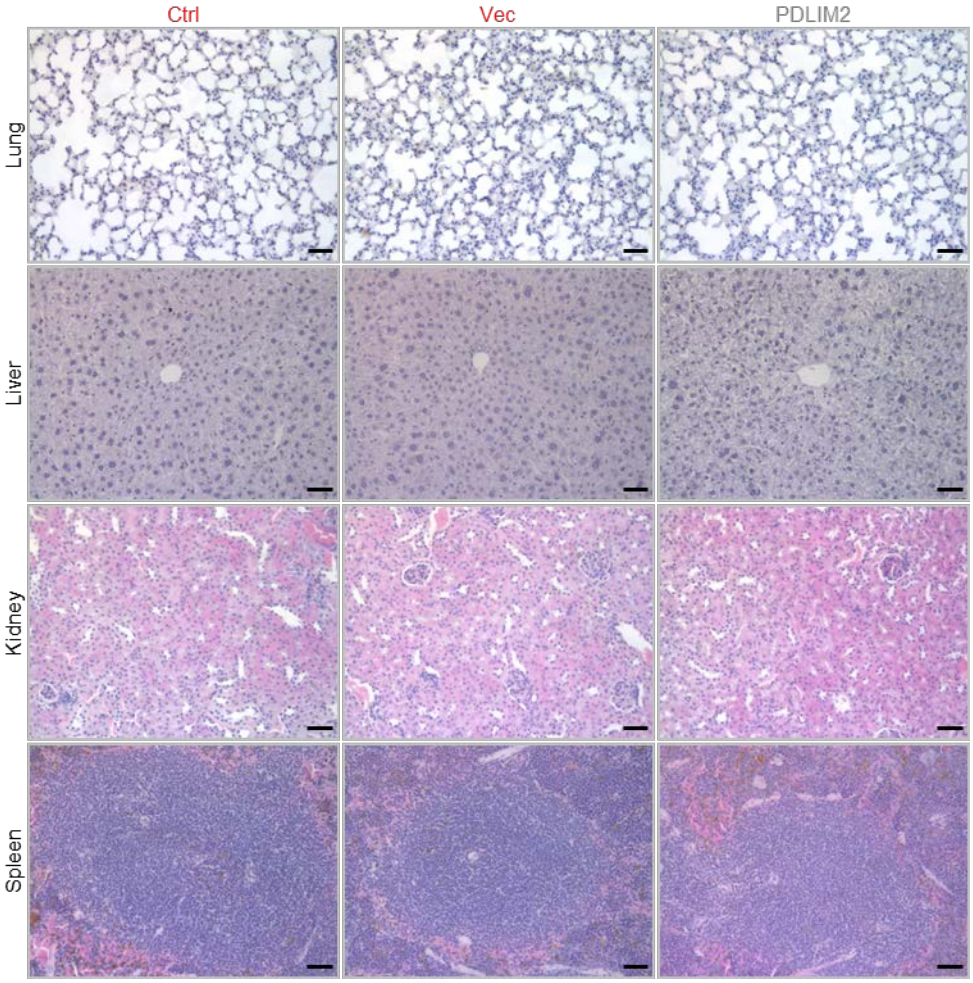

Figure S2. PDLIM2 nanotherapy causes no obvious pathological changes in major organs. H&E staining showing comparable patterns in lung, liver, kidney and spleen between Vec and PDLIM2 group in the context of combinational chemotherapy and PD-1 blockade immunotherapy (n = 5). Scale bar: 50 μm.

Supplement Figure S3

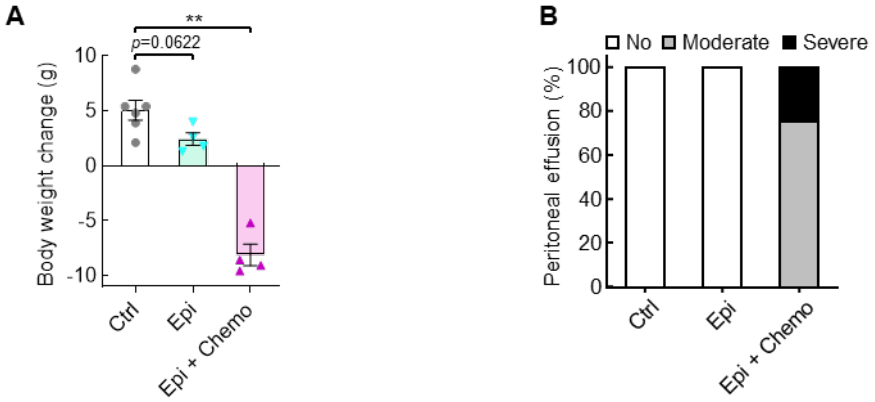

Figure S3. Epigenetic drugs cause body weight loss in mice with lung cancer. Mice were i.p. injected with urethane (1 g/kg) for 6 weeks to induce lung tumors, and then treated for 6 weeks with 5-aza-dC and MS-275 (Epi, i.p., 1 mg/kg each, twice per week), carboplatin and paclitaxel (Chemo, i.p., 30 mg/kg and 15 mg/kg, respectively, once per week), or their combinations. A, Body weight change between prior to the first treatment and the sacrifice endpoint. B, Percentage of mice with peritoneal effusion ($n \geqslant 4$).

Supplement Figure S4

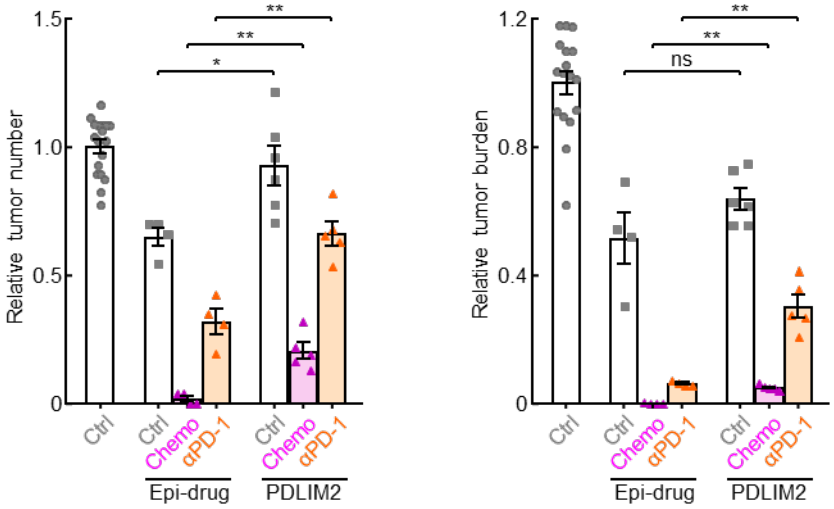

Figure S4. Epigenetic drugs show better efficacy than PDLIM2nanoparticle in lung cancer treatment. Mice were i.p. injected with urethane (1 g/kg) for 6 weeks to induce lung tumors, and then treated with 5-aza-dC and MS-275 (Epi, i.p., 1 mg/kg each, twice per week), carboplatin and paclitaxel (Chemo, i.p., 30 mg/kg and 15 mg/kg, respectively, once per week), anti-PD-1 antibody (aPD-1, i.p., 200 μg/mouse, three times per week), PDLIM2-expression plasmids containing nanoparticles (i.v., 25 μg plasmid/mouse, once per week), or their combinations for 6 weeks before they were sacrificed for tumor examination ($n \geqslant 4$).